Experiment on an Onsite Early Warning Method for the Taiwan Early Warning System

by Yih-Min Wu and Hiroo Kanamori

Introduction

As increasing urbanization is taking place worldwide, earthquake hazards pose serious threats to lives and property in urban areas. For seismic hazard mitigation, a practical earthquake forecast method appears to be far from realization, because of the extreme complexity involved in earthquake processes (e.g., Kanamori *et al.*, 1997). Another approach to mitigate seismic hazards is the development of early warning systems (EWS) (Nakamura, 1984, 1988; Heaton, 1985; United States National Research Council, 1991; Teng *et al.*, 1997; United States Geological Survey, 1998; Wu *et al.*, 1998; Wu and Teng, 2002; Allen and Kanamori, 2003). An EWS provides a few seconds to tens of seconds of warning time for impending ground motions, allowing for mitigation measures in the short term. Early warning systems that estimate the severity of ground shaking and its onset time are in operation in Japan (Nakamura, 1984, 1988, 1989), Mexico (Espinosa-Aranda *et al.*, 1995), and Taiwan (Teng *et al.*, 1997; Wu *et al.*, 1998, 1999; Wu and Teng, 2002). This timely information can be used to minimize property damage and the loss of lives in urban areas. It can also be used for real-time loss estimation to aid emergency response and recovery (Wu *et al.*, 2002).

Two types of EWS are in operation around the world. One is a front-detection EWS: seismometers installed in the earthquake source area give early warnings to more distant urban areas. Nakamura (1984) introduced the first practical system for the Japanese train system. The Taiwan and Mexico systems are examples of this type. The other is an onsite EWS, which determines the earthquake parameters from the initial portion of the *P* wave and predicts the more severe ground shakings of the following *S*-wave trains. The urgent earthquake detection and alarm system (UrEDAS) (Nakamura, 1988, 1989) is an example of this type. A prototype system, ElarmS (Allen and Kanamori, 2003) also uses this method.

In most front-detection systems, *S* waves are used for the determination of earthquake magnitude. While this method provides accurate magnitude determinations, the determination of earthquake parameters has to wait until the arrival of the *S* waves. For example, the Taiwan Central Weather Bureau (CWB) uses a front-detection system and requires an average of 22 sec to determine earthquake parameters with magnitude uncertainty of ± 0.25. It provides a warning for areas beyond about 70 km from the epicenter. In contrast, UrEDAS and ElarmS both use the predominant

period from the initial 2–4 sec of *P* waves to determine the magnitude for EWS, and the method described by Grecksch and Kumpel (1997) estimates the magnitude from the first second of the *P* wave recorded on accelerograms. However, large uncertainties in magnitude are inevitable in these methods. For ElarmS, the average absolute error in the magnitude estimate is ± 0.7, and when the closest 10 stations are used, the average error drops to ± 0.35. Grecksch and Kumpel (1997) estimate magnitudes using the rise time of the first complete peak, the predominant period, and the related Fourier amplitude of the initial part of strong-motion signals. With this approach, the magnitude uncertainty can reach as high as ± 1.35 with a single accelerogram and ± 0.5 with more than eight accelerograms.

Taiwan has established several research programs that are actively pursuing earthquake early warning and rapid reporting systems (Teng *et al.*, 1997; Wu *et al.*, 1997, 1998, 1999, 2000, 2001, 2002, 2003; Wu and Teng, 2002, 2004). The Taiwan EWS established by CWB (Fig. 1a) uses a real-time strong-motion accelerograph network consisting of 86 stations distributed around Taiwan. By applying the concept of a virtual subnetwork (VSN) to the CWB seismic network (Wu and Teng, 2002), an optimized solution between earthquake early warning and reliable magnitude determination is sought. This represents a significant step toward realistic earthquake early warning capability. The 22-sec reporting time of the Taiwan EWS will offer earthquake early warnings for metropolitan areas located more than 70 km from the epicenter. For an event with the same location as the 20 September 1999 Chi-Chi, Taiwan, earthquake, the Taipei metropolitan area, at 145 km from the epicenter, would have more than 20 sec of early warning time. Figure 1b shows the expected early warning times for an event such as the Chi-Chi earthquake for all parts of Taiwan. The small triangles give the locations of elementary schools, which essentially reflect the population density.

The idea of an early warning system presented here takes advantage of the fast data-transmission speed, which is much faster than the seismic-wave speed, and fast data-processing speed. However, the Taiwan EWS has a blind zone that gives no warning to target areas closer than 70 km from the source. To provide early warning to areas close to the source, a complementary use of an on-site EWS is desirable. Recently, Kanamori (2005) extended the method of Nakamura (1988) and Allen and Kanamori (2003) to deter-
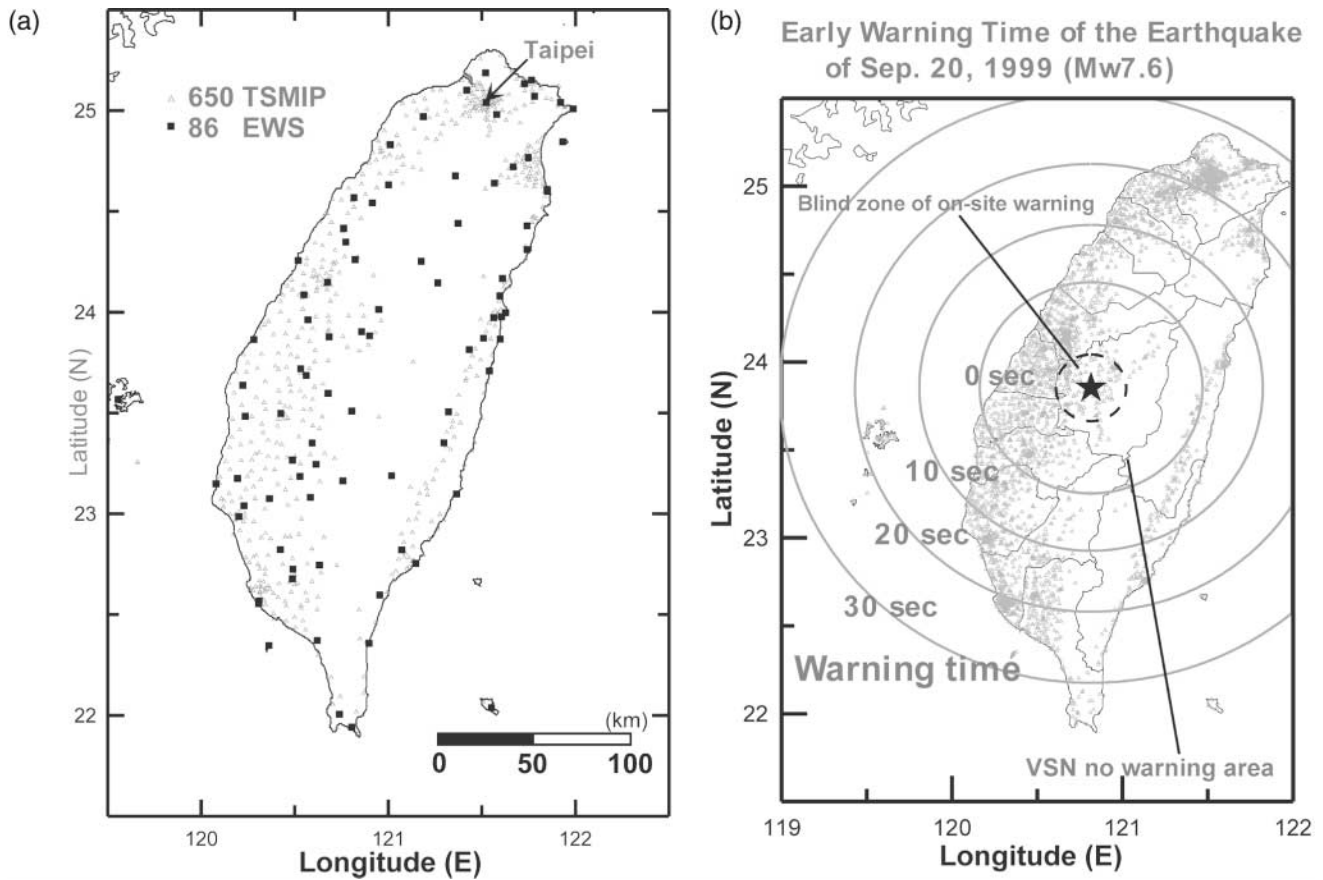
Figure 1. (a) Station distribution of the Taiwan early warning system (EWS) and the Taiwan Strong Motion Instrumentation Program (TSMIP). (b) Expected EWS early warning times (indicated by circles) in Taiwan with respect to the occurrence of an event similar to the Chi-Chi earthquake of 20 September 1999. Small circle (dashed) with a radius of 21 km indicates the boundary of the blind zone of the on-site warning method. Triangles give the locations of elementary schools, which can be regarded as an indication of the population density of Taiwan.

mine a parameter, called τ_c, that reflects the size of an earthquake from the initial 3 sec of the P waves. We have explored the use of this method to complement the front-detection Taiwan EWS system.

τ_c Method

To determine the size of an earthquake, it is important to determine whether the event's slip motion has stopped or is still growing, which is generally reflected in the period of the initial motion. Small and large events yield short- and long-period initial motions, respectively. However, the slip motion is in general complex, and even a large event often begins with a small short-period motion, followed by a long-period motion. Consequently, it is important to define the average period during the first motion, instead of the period of the first motion. The method developed by Nakamura (1988) attempts to use the period averaged over some time window. We use the following procedure, which is modified from the method used by Nakamura (1988). We take the

ground-motion displacement, $u(t)$, and velocity, $\dot{u}(t)$, from the vertical component record and compute the following ratio r by
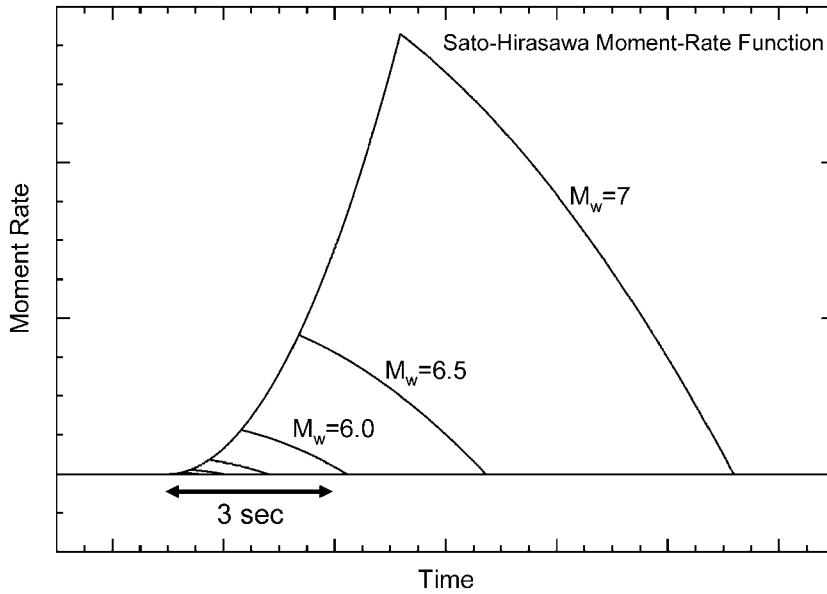
$$
r = \frac{\int_0^{\tau_0} \dot{u}^2(t)dt}{\int_0^{\tau_0} u^2(t)dt}, \tag{1}
$$

where the integration is over the time interval $(0, \tau_0)$ after the onset of the P wave. Usually, τ_0 is set at 3 sec. Using Parseval's theorem,

$$
r = \frac{4\pi^2 \int_0^{\infty} f^2 \, |\hat{u}(f)|^2 df}{\int_0^{\infty} |\hat{u}(f)|^2 df} = 4\pi^2 \langle f^2 \rangle, \tag{2}
$$

where $\hat{u}(f)$ is the frequency spectrum of $u(t)$, and $\langle f^2 \rangle$ is the average of f^2 weighted by $|\hat{u}(f)|^2$. Thus,

Numerical Test on Synthetic Source Time Function

Figure 2. Displacement waveforms computed for the kinematic source model of Sato and Hirasawa (1973). The parameters used for computation of waveforms are: *P*-wave speed, 6 km/sec; *S*-wave speed, 3.5 km/sec; density, 2.7 g/cm³; rupture speed, 2.5 km/sec; applied shear stress, 30 bars; polar angle of the station location, 90° (Kanamori, 2005).
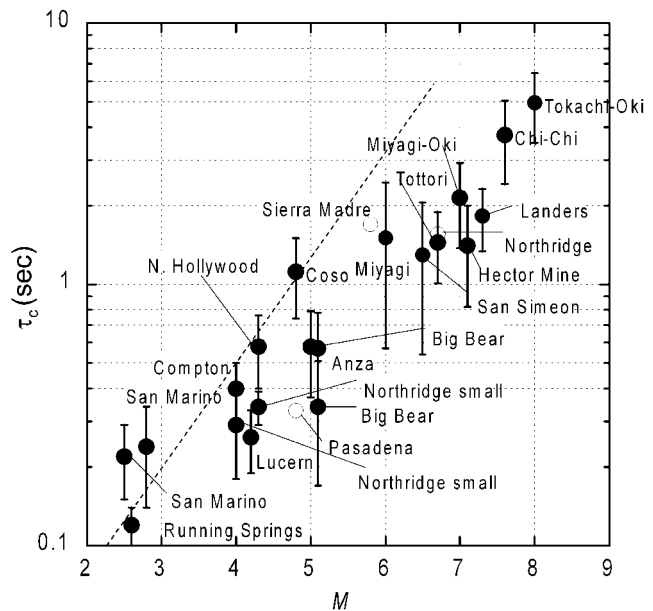
$$\tau_c = \frac{1}{\sqrt{\langle f^2 \rangle}} = \frac{2\pi}{\sqrt{r}} \qquad (3)$$

can be used as a parameter representing the period of the initial portion of the *P* wave. The larger τ_c is, the larger the event is. This method is different from Nakamura's (1988) in that we compute τ_c using the displacement *u(t)* over a fixed time window after the *P*-wave onset. To demonstrate that τ_c is a good measure of the size of an earthquake, we computed τ_c for the waveforms resulting from the kinematic source model of Sato and Hirasawa (1973). Figure 2 shows the displacement waveforms of Sato and Hirasawa's (1973) model, and τ_c computed for them using equations (1) and (3) is shown by a dashed line in Figure 3. For this particular model, τ_c saturates at M_w slightly larger than 6.5.

Kanamori (2005) has applied this method to available close-in records for events with *M* 2.5 to 8.0 (the 2003 Tokachi-Oki, Japan, earthquake) to determine τ_c. As shown in Figure 3, the results are consistent with the simulation result for the model of Sato and Hirasawa (1973) shown by the dashed line. The difference in the slope is due to the difference in the source time functions between the model of Sato and Hirasawa (1973) and the real earthquakes. Somewhat surprisingly, τ_c keeps increasing even for earthquakes with *M* >7, without any obvious sign of saturation. Since the data set is sparse for very large events (only five earthquakes with *M* ≥7), this result is not conclusive.

For the EWS application, if τ_c < 1 sec, the event has already ended or is not likely to grow beyond *M* >6. If τ_c > 1 sec, it is likely to grow, but how large it will eventually become cannot be determined. In this sense, this method provides a threshold warning.

Figure 3. τ_c computed for earthquakes with 2.5 < *M* < 8.0 in Japan and California using close-in seismograms (Kanamori, 2005). *M* represents M_w and M_L for *M* ≥6, and *M* <6, respectively. Open circles indicate data points for which only one or two records were available. The error bars indicate one standard deviation.

Data and Analysis

Large and shallow earthquakes often cause the most serious damage. Thus, we selected 26 events in Taiwan for this study (Table 1). The selection criteria were M_w >5.0 and focal depth <35 km, as listed in the Harvard catalog.

All the events were well recorded by the Taiwan Strong Motion Instrumentation Program (TSMIP) network. These events occurred during the period from 1993 to 2003 and were widely felt in Taiwan. With about 650 modern digital accelerographs installed at free-field sites (Fig. 1a), the TSMIP station signals are digitized at 200 samples per second or higher at 16-bit resolution. Most accelerographs have a dynamic range of ± 2 g.

A total of 507 TSMIP records were used for this study. They were recorded at an epicentral distance of less than 30 km, and at least eight records were available for each event. For EWS purposes, near-source records are most important.

Vertical component strong-motion records were used in this study. Input signals were integrated twice to displacement records. We applied a 0.075-Hz high-pass Butterworth filter to remove the low-frequency drift after integration. We used an automatic P picker similar to that described by Allen (1978) to detect the P-wave arrival from vertical acceleration records. In this study, we computed τ_c from the 3-sec-long filtered displacement signals after the P arrival. We also computed the peak displacement amplitude (PK3s) for the same time window for further analysis.

Results

Figure 4a shows τ_c determined from all of the 507 records plotted as a function of M_w. Although log τ_c increases

approximately linearly with M_w, the scatter is very large, especially for events with M_w <5.5. The large scatter is primarily due to the very small displacement amplitudes, PK3s, during the first 3 sec. Figure 4b shows PK3s for all of the 507 records as a function of M_w. The initial amplitude PK3s is generally small for the smaller events, especially for events with M_w <5.5; this results in a poor signal-to-noise
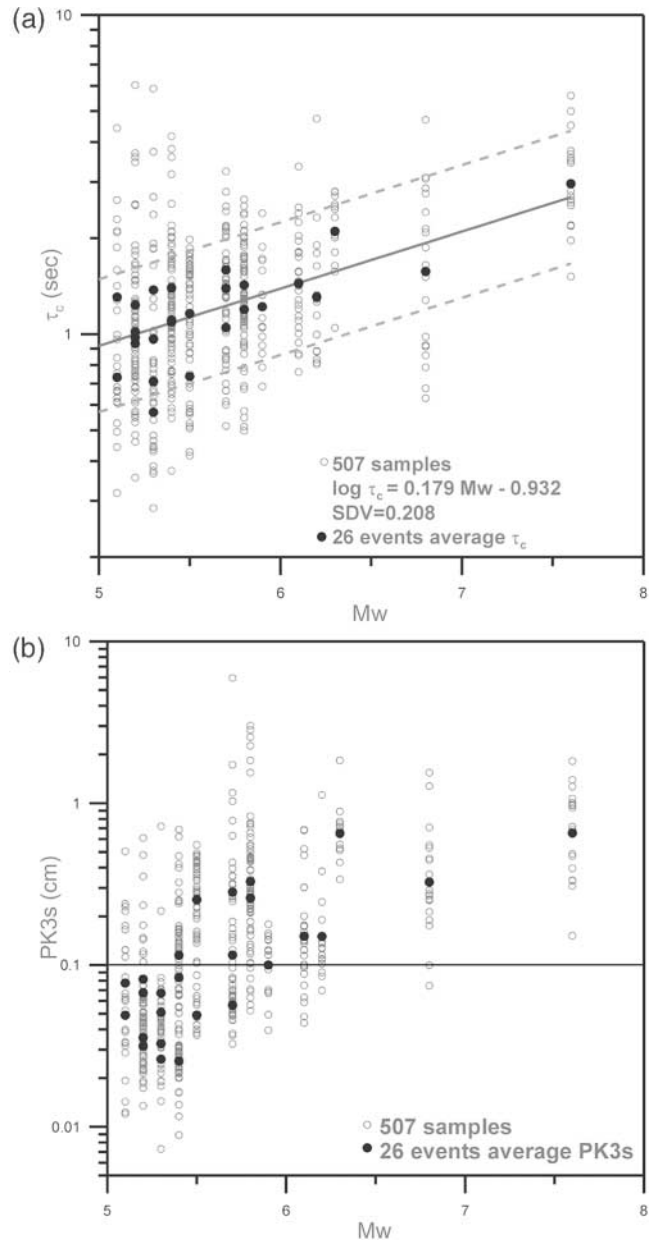

Figure 4. (a) τ_c measurements (open circles) from 507 strong-motion records within the epicentral distance of 30 km versus M_w. Solid circles show the average for the 26 events listed in Table 1. (b) PK3s measurements from 507 strong-motion records within the epicentral distance of 30 km versus M_w. Solid circles show the average for the 26 events listed in Table 1.

Table 1
Twenty-six Events Used in This Study

No.	Origin Time (UT)		Lat. (N)	Long. (E)	Depth (km)	M_w	No. of Records
1	1993/12/15	21:49:43.10	23.213	120.524	12.50	5.4	26
2	1994/06/05	01:09:30.09	24.462	121.838	5.30	6.3	13
3	1995/01/10	07:55:19.56	23.680	121.432	3.81	5.1	14
4	1995/02/23	05:19:02.78	24.204	121.687	21.69	6.2	16
5	1995/05/27	18:11:11.12	23.008	121.465	19.73	5.7	8
6	1995/12/18	16:17:54.53	24.018	121.692	22.06	5.2	22
7	1996/11/26	08:22:23.71	24.164	121.695	26.18	5.2	16
8	1998/01/18	19:56:51.71	22.725	121.089	3.28	5.2	18
9	1998/07/17	04:51:14.96	23.503	120.663	2.80	5.7	27
10	1998/11/17	22:27:32.52	22.832	120.790	16.49	5.3	10
11	1999/09/20	17:47:15.85	23.855	120.816	8.00	7.6	18
12	1999/10/22	02:18:56.90	23.517	120.423	16.59	5.8	43
13	1999/10/22	03:10:17.46	23.533	120.431	16.74	5.5	43
14	1999/10/30	08:27:49.50	24.017	121.319	14.36	5.4	22
15	2000/02/15	21:33:18.15	23.316	120.740	14.71	5.2	16
16	2000/07/14	00:07:32.46	24.048	121.728	7.19	5.4	29
17	2000/08/23	00:49:16.58	23.636	121.635	27.48	5.3	11
18	2000/09/10	08:54:46.53	24.085	121.584	17.74	5.8	31
19	2001/06/14	02:35:25.78	24.419	121.928	17.29	5.9	15
20	2001/06/19	05:16:15.46	23.177	121.077	6.58	5.3	11
21	2001/06/19	05:43:39.17	23.197	121.098	11.70	5.1	13
22	2002/02/12	03:27:25.00	23.741	121.723	29.98	5.7	21
23	2002/04/03	18:06:10.79	24.322	121.868	12.87	5.3	9
24	2002/05/15	03:46:05.91	24.651	121.872	8.52	6.1	26
25	2003/06/16	18:33:38.85	23.543	121.654	28.26	5.5	10
26	2003/12/10	04:38:13.52	23.067	121.398	17.73	6.8	19

ratio for τ_c determinations. From the EWS point of view, small-amplitude data are not of interest, and also τ_c needs to be determined as rapidly as possible after the *P* wave is detected at the first station. Thus, in our experiment we removed all of the data with PK3s < 0.1 cm and used only the first eight stations within less than 21 km to determine τ_c. Figure 5a shows the results for which the first eight records with PK3s > 0.1 cm are used. The determinations were made for the 12 events for which such data were available. Table 2 summarizes the results of τ_c determinations

together with the distance to the farthest station. The relationship between the average τ_c and M_w is given by,

$$\log\tau_c = 0.221M_w - 1.113 \qquad (4)$$

or, conversely, by,

$$M_w = 4.525\log\tau_c + 5.036 \qquad (5)$$

The earthquakes we studied all had $M_w > 5$ and were potentially damaging; except for one earthquake, all of them
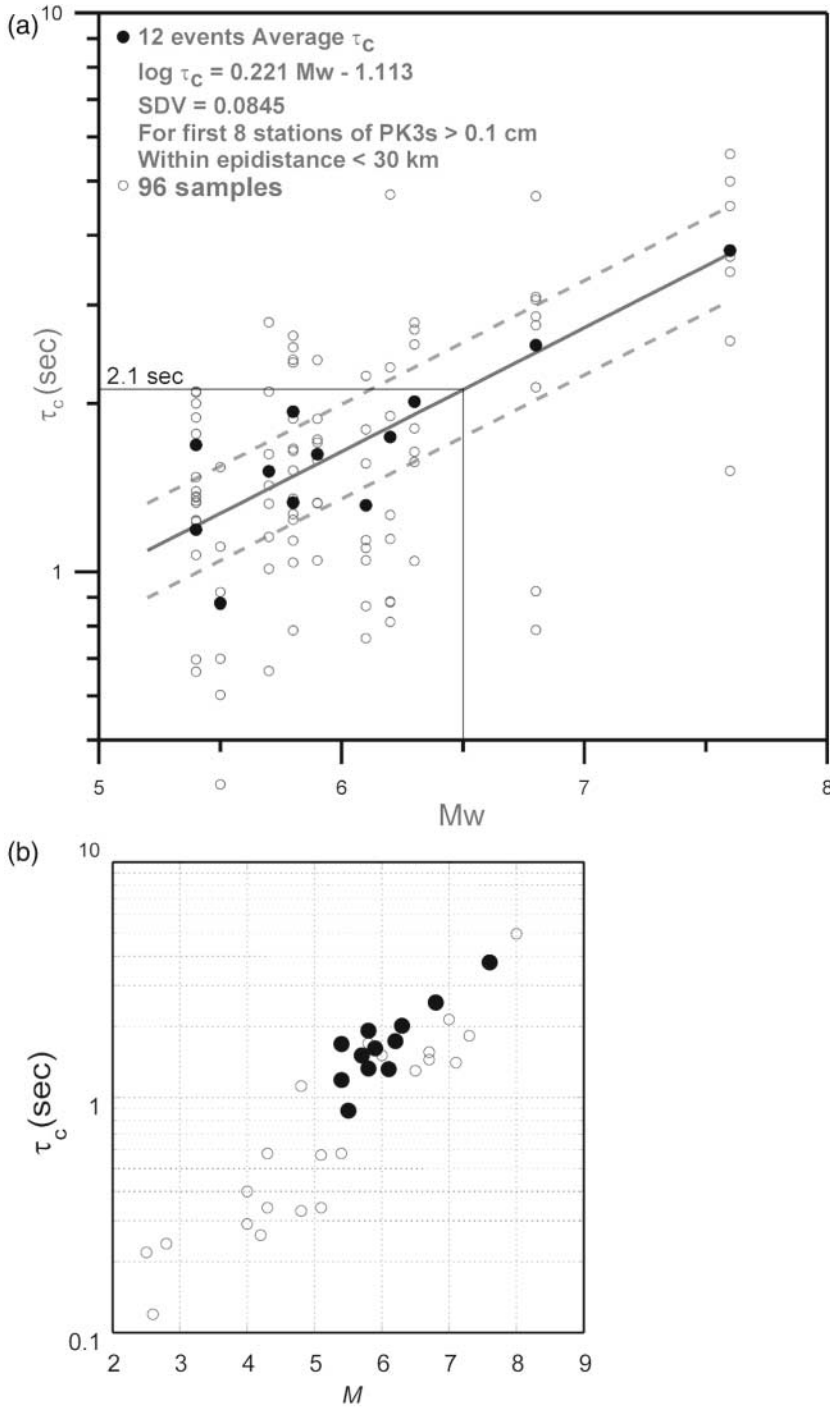

Figure 5.   (a) Relationship between the averaged τ_c and M_w of the 12 events from the closest eight records with PK3s > 0.1 cm. (b) The average τ_c determined for the Taiwan events shown in Figure 5a (solid circles) together with those for earthquakes in Japan and California (open circles). The definition of *M* is the same as that in Figure 3.

Table 2
τ_c of 12 Events from Closest Eight Records with PK3s > 0.1 cm

No.	M_w	τ_c	τ_c 1	τ_c 2	τ_c 3	τ_c 4	τ_c 5	τ_c 6	τ_c 7	τ_c 8	Dist
1	5.4	1.19	1.77	1.36	0.66	1.34	1.39	0.7	1.23	1.07	20.5
2	6.3	2.02	1.05	1.64	1.57	2.79	1.81	2.71	2.01	2.55	19.9
4	6.2	1.74	0.89	4.73	0.81	1.26	2.32	0.88	1.14	1.90	19.4
9	5.7	1.51	2.10	1.43	1.01	2.80	1.62	1.32	1.15	0.66	20.1
11	7.6	3.76	5.00	3.66	3.76	5.59	4.51	2.59	3.44	1.52	20.4
12	5.8	1.93	2.64	1.88	2.52	1.52	2.37	2.40	0.79	1.35	20.6
13	5.5	0.88	0.42	0.88	0.87	0.60	0.92	0.70	1.54	1.11	20.6
16	5.4	1.69	1.89	1.48	2.09	2.10	1.36	1.24	1.33	2.00	20.4
18	5.8	1.33	1.24	1.33	1.14	1.66	1.27	1.04	1.32	1.65	20.4
19	5.9	1.62	1.70	1.05	1.88	1.58	1.33	2.39	1.72	1.33	20.7
24	6.1	1.32	2.24	1.80	0.87	1.10	0.76	1.56	1.05	1.14	19.9
26	6.8	2.54	4.70	3.10	2.76	3.07	2.86	0.92	2.14	0.79	18.2

τ_c, average value for each event unit in s; τ_c 1–8, τ_c for the closest eight stations; Dist, epicentral distance in kilometers of the eighth closest station.

Figure 6.   Rapid reporting time and warning distance of the τ_c and VSN methods.

had $\tau_c > 1$ sec. As shown in Figure 5b, this trend is consistent with that obtained for the events in Japan and California (Figure 3).

For events in California, broad-band records were used for small events, and most events with $M_w < 5$ have $\tau_c > 1$ sec. Thus, the use of τ_c provides a useful threshold warning for large earthquakes. If $\tau_c > 1$ sec, the event is potentially damaging. If it is larger than 2 sec, the event is almost certainly damaging. Combining this information with other data, such as the initial velocity and displacement amplitudes, would allow the damage potential of the event to be assessed more accurately.

Discussion and Conclusions

In Taiwan, the TSMIP telemetered stations are densely distributed all over the island. If detection of the P arrival and the determinations of τ_c and PK3s are made on-site, these parameters can be sent to the control center rapidly and reliably. By using the average of the values from the first eight stations as an indicator, earthquake early warnings can be issued rapidly. Furthermore, Internet function can now be installed at most sites, which will save much of the telemetry cost.

Figure 6 shows the travel time of P and S waves for a reference focal depth at 10 km. Currently the Taiwan EWS can provide rapid reporting at 22 sec after the event origin time by using the VSN method. The 2003 Chengkung M_w 6.8 earthquake is a representative case. The VSN system reported the information on this earthquake at 22 sec after the occurrence with an estimated M_L of 6.5 and a good hypocenter determination. The front-detection EWS provides a warning to areas at distances greater than about 70 km from the epicenter (i.e., the radius of the blind zone is 70 km). In our experiment on the τ_c method, we used P waves from the strong-motion records within 21 km of the epicenter. Figure 6 shows that P waves need about 4.5 sec to reach 21 km. And this method needs only 3 sec of waveform data.
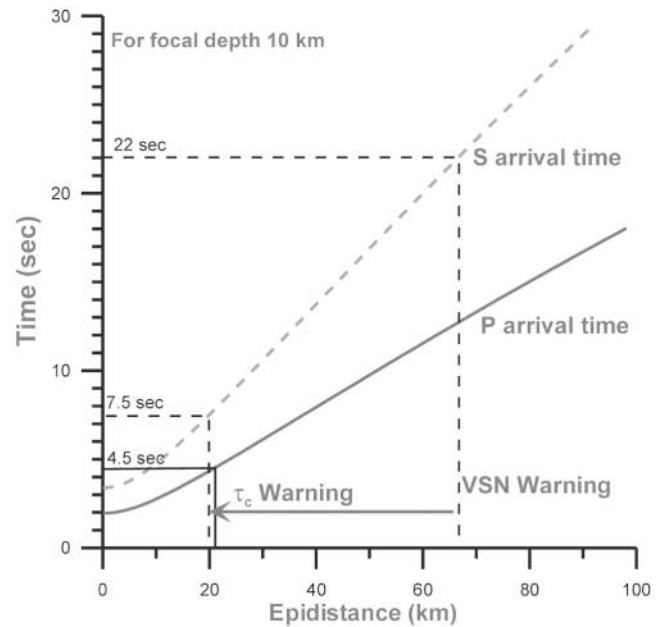
Thus, the total procedure needs about 7.5 sec. At that time, S waves have propagated only to about 20 km from the epicenter, so we can reduce the radius of the blind zone to 20 km (Fig. 1b).

Large damaging earthquakes with very large ground motions often caused interruption of telemetry within a few seconds after the onset, resulting in the loss of data. This problem caused difficulty in the traditional measurement of peak amplitude for determination of M_L and intensity. However, the τ_c method can overcome this difficulty because τ_c and PK3s are measured from the beginning of P arrival, before telemetry interruption occurs.

Our experiment on the τ_c method using the data in the Taiwan region suggests that it is possible to determine, on-site, both τ_c and PK3s, which jointly give reliable threshold warnings. The τ_c method can reduce the radius of the blind zone to 20 km, and it will be a useful complement to the front-detection EWS in Taiwan.

Acknowledgments

References

Allen, R. V. (1978). Automatic earthquake recognition and timing from single traces, *Bull. Seism. Soc. Am.* **68,** 1521–1532.
Allen, R. M., and H. Kanamori (2003). The potential for earthquake early warning in Southern California, *Science* **300,** 685–848.

Espinosa-Aranda, J., A. Jiménez, G. Ibarrola, F. Alcantar, A. Aguilar, M. Inostroza, and S. Maldonado (1995). Mexico City seismic alert system, *Seism. Res. Lett.* **66,** 42–53.

Grecksch, G., and H. J. Kumpel (1997). Statistical analysis of strong-motion accelerogram and its application to earthquake early-warning systems, *Geophys. J. Int.* **129,** 113–123.

Heaton, T. H. (1985). A model for a seismic computerized alert network, *Science* **228,** 987–990.

Kanamori, H. (2005). Real-time seismology and earthquake damage mitigation, *Annu. Rev. Earth Planet. Sci.* (in press).

Kanamori, H., E. Hauksson, and T. Heaton (1997). Real-time seismology and earthquake hazard mitigation, *Nature* **390,** 461–464.

Nakamura, Y. (1984). Development of the earthquake early-warning system for the Shinkansen, some recent earthquake engineering research and practical in Japan. The Japanese National Committee of the International Association for Earthquake Engineering, 224–238.

Nakamura, Y. (1988). On the urgent earthquake detection and alarm system (UrEDAS), *Proc. of the 9th World Conference on Earthquake Engineering,* Tokyo-Kyoto, Japan.

Nakamura, Y. (1989). Earthquake alarm system for Japan railways, *Jpn. Railway Eng.* **109,** 1–7.

Sato, Y., and Y. Hirasawa (1973). Body wave spectra from propagating shear cracks, *J. Phys. Earth* **21,** 415–431.

Teng, T. L., Y. M. Wu, T. C. Shin, Y. B. Tsai, and W. H. K. Lee (1997). One minute after: strong-motion map, effective epicenter, and effective magnitude, *Bull. Seism. Soc. Am.* **87,** 1209–1219.

United States Geological Survey (1998). *A plan for implementing a real-time seismic hazard warning system.* A report to Congress required by public law 105-47. 27 March 1998, Washington, D.C.

United States National Research Council (1991). Real-time earthquake monitoring, Report from the Committee on Seismology, National Academy Press, Washington, D.C., USA. 52 pp.

Wu, Y. M., and T. L. Teng (2004). Near real-time magnitude determination for large crustal earthquakes, *Tectonophysics* **390,** 205–216.

Wu, Y. M., and T. L. Teng (2002). A virtual sub-network approach to earthquake early warning, *Bull. Seism. Soc. Am.* **92,** 2008–2018.

Wu, Y. M., C. C. Chen, T. C. Shin, Y. B. Tsai, W. H. K. Lee, and T. L. Teng (1997). Taiwan Rapid Earthquake Information Release System, *Seism. Res. Lett.* **68,** 931–943.

Wu, Y. M., T. C. Shin, and Y. B. Tsai (1998). Quick and reliable determination of magnitude for seismic early warning, *Bull. Seism. Soc. Am.* **88,** 1254–1259.

Wu, Y. M., J. K. Chung, T. C. Shin, N. C. Hsiao, Y. B. Tsai, W. H. K. Lee, and T. L. Teng (1999). Development of an integrated seismic early warning system in Taiwan—case for the Hualien area earthquakes, *TAO: Terrestrial, Atmospheric and Oceanic Sciences* **10,** 719–736.

Wu, Y. M., W. H. K. Lee, C. C. Chen, T. C. Shin, T. L. Teng, and Y. B. Tsai (2000). Performance of the Taiwan Rapid Earthquake Information Release System (RTD) during the 1999 Chi-Chi (Taiwan) earthquake, *Seism. Res. Lett.* **71,** 338–343.

Wu, Y. M., T. C. Shin, and C. H. Chang (2001). Near realtime mapping of peak ground acceleration and peak ground velocity following a strong earthquake, *Bull. Seism. Soc. Am.* **91,** 1218–1228.

Wu, Y. M., N. C. Hsiao, T. L. Teng, and T. C. Shin (2002). Near real-time seismic damage assessment of the rapid reporting system, *TAO: Terrestrial, Atmospheric and Oceanic Sciences* **13,** 313–324.

Wu, Y. M., T. L. Teng, T. C. Shin, and N. C. Hsiao (2003). Relationship between peak ground acceleration, peak ground velocity, and intensity in Taiwan, *Bull. Seism. Soc. Am.* **93,** 386–396.

Department of Geosciences
National Taiwan University
No. 1, Sec. 4, Roosevelt Road
Taipei 106, Taiwan
drymwu@ntu.edu.tw
    (Y.M.W.)

Seismological Laboratory
California Institute of Technology
Pasadena, California 91125
    (H.K.)